

Temperature Measurement System for the Mixture of Capric Acid and Lauric Acid as a Low-Temperature Thermal Energy Storage Medium

Maria Natalia R. Dimaano^{1§} and Takayuki Watanabe²

¹*Faculty of Engineering and
Research Center for the Natural Sciences
University of Santo Tomas
España, Manila 1008 Philippines*

²*Research Laboratory for Nuclear Reactors
Tokyo Institute of Technology
2-12-1 O-okayama, Meguro-ku
Tokyo, 152-8550 Japan*

Abstract. The mixture of capric acid and lauric acid (C-L acid mixture), as a latent heat storage material, is placed in a vertical copper tube that is coaxially fixed in a cylinder containing water that serves as the heat transfer fluid. The temperature distribution in the C-L acid in both radial and axial directions is measured using a Type K thermocouple probe set-up. The heat flux during melting of the C-L acid is determined to confirm the reliability of the temperature measurement and storage system set-up. The radial temperature measurement exhibits the expected interfacial distribution in the C-L acid. Results fare off well in terms of heat flux in the 0, 100, and 200 mm probe height positions.

Key words: Thermal energy storage, latent heat storage material, C-L acid mixture, phase change material, thermocouple probe, storage capsule.

INTRODUCTION

Thermal energy storage systems have gained considerable merits due to the demand to completely phase out the use of ozone-depleting refrigerants and due to the need for energy conservation. It offers capital cost savings on premium fuels and cost effectiveness due to the reduction of energy wastage.

§Author to whom correspondence should be addressed.

Among the technologies available, the latent thermal energy storage system offers the greatest energy storage density, accommodating a large amount in a relatively compact storage unit. It exhibits a small temperature swing and requires minimal insulation. Solid to liquid phase change materials are used as thermal energy storage media that can store the needed amount of energy and later on collect heat from a space unit. These materials lower the temperature to a comfortable climatic characteristic and rejects the collected heat from this space unit through convection.

However, heat transfer in latent heat storage materials is usually complicated by the phase change that occurs during the absorption or release of energy. Considerable attention has been made on the melting and solidification phase transition phenomena of various storage media. Hamdan and Elwerr [1] investigated the 2-dimensional melting process of a solid PCM contained in a rectangular enclosure, while Gong [2] carried out an extended investigation of enhancing melting and solidification heat transfer using composite slabs with different melting temperatures. Farid [3] studied three types of PCM with different melting temperatures employing air as the heat transfer fluid, and Watanabe [4] augmented the system performance by using water as the heat transfer fluid. Masuoka [5] proposed a composite of naphthalene with copper fiber for an increased thermal diffusivity in the storage medium and a reduction in supercooling during its solidification. Feldman [6] determined the melting and solidification characteristics of esterified different mixtures of fatty acids using the DSC method. Several storage modules had been proposed to evaluate the suitability of the phase change materials for thermal energy storage. Kim [7] experimentally studied glauber's salt with celite in an enclosed vertical cylinder with a hot transfer fluid flowing through a copper tube fixed at the center of the PCM cylinder. Carlsson [8] studied calcium chloride hexahydrate ($\text{CaCl}_2 \cdot 6\text{H}_2\text{O}$) using a vertical single pipe heat exchanger tube placed centrally along the axis of the cylinder. This work was extended by Yanadori [9] using a vertical double pipe heat exchanger which led to the establishment of a new experimental equation which they considered useful for thermal design of heat storage containers. Kemink [10] did a comprehensive study on the measurement of heat transfer coefficients for melting about a vertical cylinder embedded in n-eicosane paraffin whose temperature was either in its melting point or subcooled below its melting value. There were even more sophisticated models done by Brosseau [11] and Aceves [12], to cite a few. Brosseau predicted the thermal behavior of a PCM inside a multilayer storage unit while Aceves optimized the performance characteristics of the energy storage composed of multiple energy storage cell with multiple PCMs. The vertical cylinder is employed in this paper because of its simplicity in structure and easy handling.

A particularly interesting phase change material that is being considered for low temperature thermal energy storage in the Philippines is the mixture of 65% Capric Acid and 35% Lauric Acid by mole composition (C-L acid mixture) [13]. Capric acid and lauric acid can be derived from coconut oil [14] and are hence easily available. An alternative source of capric acid is goat oil [15] which is also abundant in the Philippines.

It is the objective of this study to measure the radial and axial temperature distribution during the melting of the C-L acid mixture. A temperature measurement system was assembled to monitor the temperature during the various stages of phase transition. The results of these measurements will provide a basis for the evaluation of the performance of the heat storage system.

EXPERIMENTAL

Phase change material. A mixture composed of 65 mole% capric acid and 35 mole% lauric acid was used as a storage material. Both fatty acids have 98% purity, as manufactured by Tokyo Chemicals, Inc. The melting characteristics of the mixture obtained from DSC analysis using the TA Instrument DSC 2010 provided a melting temperature range of 18-20 °C and a heat of fusion of 148.0 kJ/kg.

Temperature measurement system. The temperature measurement system was based on the fabricated Chromel-Alumel (Type K) thermocouples. Each chromel and alumel wire has a diameter of 0.28 mm and coated with an insulator. The wires were joined together in one end by gas welding with the sensing junction beads finally formed to diameters ranging from 0.6 to 0.9 mm. Each thermocouple was individually calibrated for higher accuracy assurance, showing a $\pm 0.68\%$ deviation against established Type K standard.

Figure 1 shows the probe sensor set-up designed for the radial temperature measurement in the C-L acid mixture. It was made up of 2 rectangular acrylic slabs, each having 10 holes to hold the thermocouple probes and an acrylic pipe to support the thermocouple wires. The holes were positioned at a distance of 1.5, 4.5, 7.5, 10.5, and 13.5 mm on both sides from the center of the slab. A thermocouple probe was fitted in each hole. This probe assembly is used to determine the radial temperature distribution in the C-L acid throughout the melting process.

Heat storage module. The heat storage module consists of an annular acrylic cylinder with both ends sealed with an acrylic board. The upper end had a hole ($\phi \approx 33\text{mm}$) through which was inserted the copper tube encapsulating the PCM and the probe assembly. The vertical copper tube was fixed vertically in the

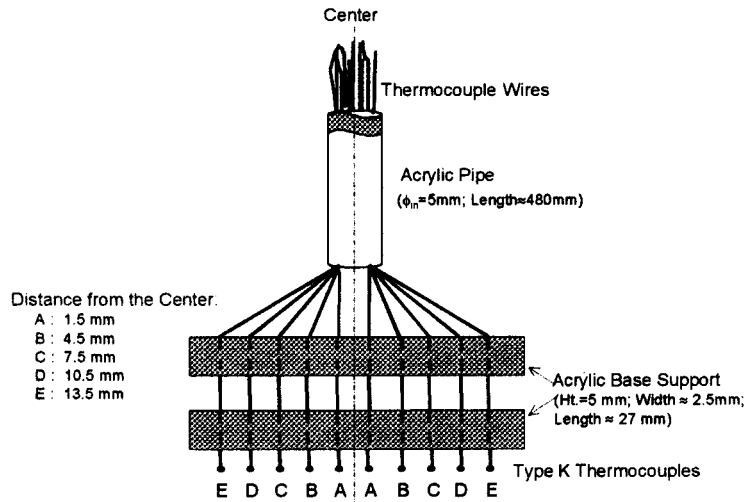


Figure 1. Chromel-alumel thermocouple probe

center of the cylinder. Inlet and outlet holes were bored on opposite sides 5 mm from both ends of the acrylic cylinder. A sketch of the heat storage module used in this study is presented in Figure 2.

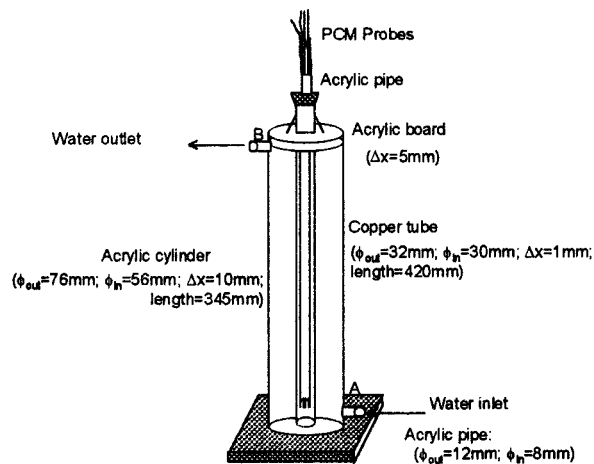


Figure 2. A vertical coaxial tubular heat exchange system (storage capsule).

Water serving as the heat transfer fluid, flows through the annular cylinder with its temperature monitored by the thermocouple probes set at the inlet (A) and outlet (B) of the storage module. The position of the thermocouple probe assembly could be varied by setting it at height positions of 0, 100, 200, and 300 mm from the base of the copper tube. At each position, the probe assembly measures the radial temperature distribution at positions of 1.5, 4.5, 7.5, 10.5, and 13.5 mm in both directions away from the center.

Experiment set-up. A schematic of the experimental set-up is presented in Figure 3. A heater/cooler waterbath with pump and temperature controller is used for the charging and discharging processes. The storage capsule and pipes are wrapped with fiberglass and/or asbestos mat thermal insulators to reduce the heat leakage to the air.

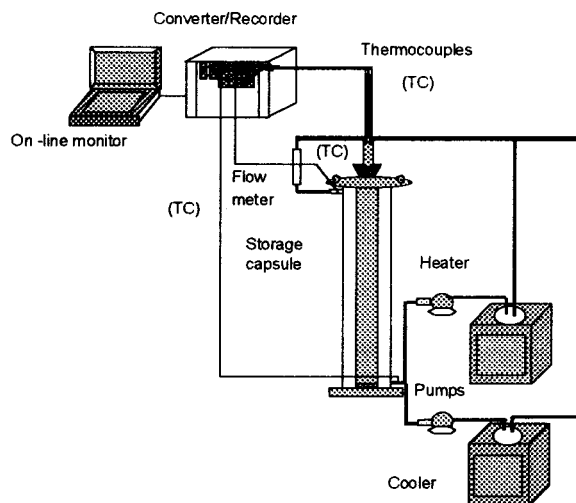


Figure 3. A schematic diagram of the experimental set-up.

The thermocouples are connected to a PC based electronic data acquisition/sampling system using the multiple converter Yew Model 3081 Hybrid Recorder. The probe assembly was initially set at the designated height position. The C-L acid mixture is initially solidified before it is subjected to the melting process. Solidification is achieved with inlet water temperature kept at 7°C, while melting is performed with 40°C of inlet water temperature. Temperature measurements are taken at time interval of 6 seconds. Each experiment ends as soon as all the radial temperature in the C-L acid mixture approaches the temperature of water that is maintained at a constant flowrate of $1.67 \times 10^{-5} \text{ m}^3/\text{s}$.

RESULTS AND DISCUSSION

Figure 4 shows the radial temperature distribution in the C-L acid mixture during the melting process monitored at different axial positions. The melting band represents the phase transition region establishing the optimum melting range. It was derived from 90% of the total height of the endotherm obtained from the DSC analysis. The total height is the vertical measurement of the thermal event from its baseline to its melting peak. The melting peak corresponds to the maximum phase transition activity in the phase change material. Below the melting band is the solid region and above the melting band is the liquid region.

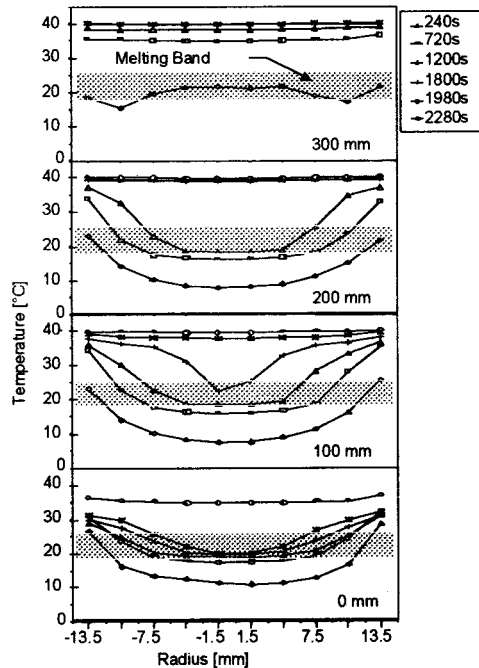


Figure 4. Radial melting temperature profile of C-L acid at different probe height positions relative to the base.

At the early stage of the charging process, a concave radial temperature distribution was obtained with higher temperature occurring at the outermost radius and lower temperature towards the center. This curve illustrates the distribution in the liquid, liquid transition, and solid regions of the C-L acid. While complete melting was not yet attained, a thermal lag persisted along the inner radii. This behavior was observed in the radial melting profile at all heights, except 300mm, particularly that which was monitored at 0 mm probe height position wherein the concave curves were formed from 240s until 1980s. The outer radius temperature was generally above the melting band that depicted an instantaneous complete melt, further showing that melting started at the outer radius towards the inner radii of the PCM.

As the charging proceeded, the temperature of the inner radii increased within the melting band, correspondingly with a simultaneous rise in temperature in higher layers of the PCM. At a height of 300mm, the temperature of the whole layer at 240s was within the melting band showing that the PCM layer quickly melted. At a longer charging time, the radial temperature distribution flattened relatively becoming earlier at higher heights (i.e., 2280s at 0 mm, 1980s at 100 mm, 1800s at 200 mm, and 1200s and 720s at 300 mm height positions). This characterized the axial melting behavior of the C-L acid that proceeded from top to bottom of the storage capsule. As a whole, a general symmetry in the radial temperature profile presents an effective temperature probe set-up.

Figure 5 shows the variation with time of the inlet and outlet water temperatures and the radial temperature history of the C-L acid as it undergoes the melting process. It took 24s for the inlet water to completely adapt and correspond to the set temperature of water in the circulating waterbath from the initially sustained temperature in the storage capsule. A 30 °C difference between the inlet and outlet water temperature was observed at the early stage of the charging process. This is due to the contained amount of energy in the PCM that maximally absorbed the heat lost by water from the onset of charging until 240s. In 180 mins., the outlet water temperature became nearly constant and stabilized, approaching the temperature of inlet water.

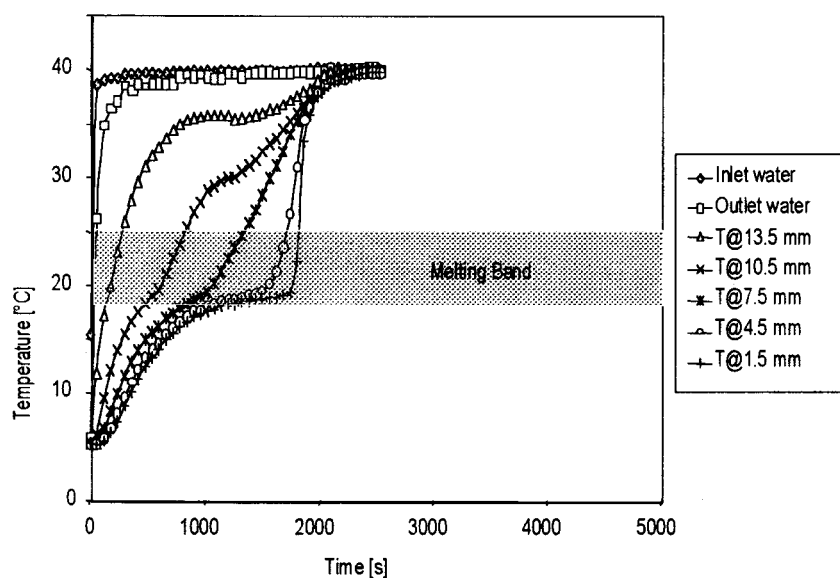


Figure 5. C-L acid melting temperature history at five different radial positions monitored at 100mm probe height position.

The temperature rise at different radial positions varied in the C-L acid, being faster at the outer radial position and slower on the inner radii. The supply of heat was faster on the outer radii. The outer radius reached the melting band first and consequently followed by the adjacent inner radii. Due to their distance from the heat source, the supply of heat was slower in the inner radii thus took longer time to reach the melting band. The C-L acid temperature leveled off at the time when the inlet and outlet water temperature difference stabilized. This is particularly seen in the 7.7 mm, 10.5 mm, and 13.5 mm radial positions implying that melting dominantly took place in the range 18-20 °C. Right after complete melting in the C-L acid was achieved, the radial temperature

continuously increased and rapidly approached the inlet water temperature. The complete melting time of the C-L acid was 1720s, estimated from the time when the outermost radius reached the lower temperature limit of the melting band until the innermost radius attained the highest temperature limit in the melting band.

With these results, the transient temperature distribution in the C-L acid during its melt provides the necessary information on the actual time-dependence of its location and shape. The repeatability of the data at the same temperature range and probe positions ruled out the possible errors on hysteresis which are difficult to predict. Furthermore, it established the confidence in the probe set-up and confirmed its adaptability to further elucidate the characteristic behavior of the C-L acid mixture.

$$\frac{\underline{Q}}{A} = \frac{\dot{m} \times C_p \times \int_0^t (T_{in} - T_{out}) dt}{A}$$

Further evaluation on the efficiency of temperature measurement design was tackled by the estimation of the heat flux of the C-L acid mixture at different probe height positions. The heat flux of water to the C-L acid mixture is defined from the relation.

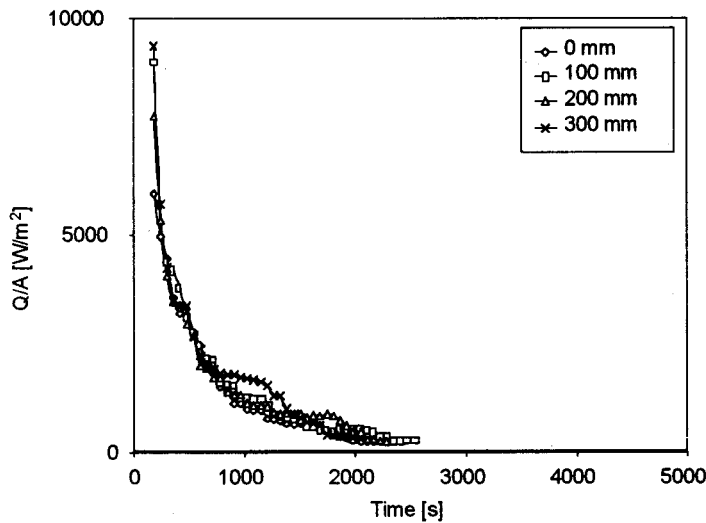


Figure 6. Melting heat flux of C-L acid at different probe height positions with 40°C inlet water temperature.

Figure 6 shows the heat fluxes along the axial position of the mixture. Although the 300mm height positioned probe manifested a slight deviation in the heat flux accounted from natural experimental nuances (*i.e.*, dropping down of solids during melting), the similarity in the values obtained nevertheless inferred the effectiveness of the measurement system design.

CONCLUSION AND RECOMMENDATION

The results obtained in this observation are useful information about the melting behavior of the C-L acid mixture. The radial and axial temperature distribution in the C-L acid mixture has been established, measured by Type K thermocouple sensors and employed in vertical cylindrical storage capsules, corroborating with the typical and well founded stepwise change during phase transition. It concurs the applicability of this temperature measurement system for the study of probable storage materials' thermal characteristics evaluation and heat storage performance as a whole.

ACKNOWLEDGMENT

This research was carried out through the joint support granted by the Japan Society for the Promotion of Science (JSPS), the Philippine Department of Science and Technology, Tokyo Institute of Technology and the University of Santo Tomas.

Nomenclature

A	lateral area of the system [m^2]
C_p	specific heat of water [(KJ)/kg-K]
\dot{m}	mass flow rate of water [kg/s]
Q	heat flow [W]
T_{in}	temperature of inlet water [K]
T_{out}	temperature of outlet water [K]
t	time [s]

REFERENCES

- [1] M. A. Hamdan and F. A. Elwerr. *Solar Energy*. **56** (2) (1996) 183.
- [2] Z. X. Gong and A. S. Mujumdar. *International Journal of Heat and Mass Transfer*. **39** (4) (1996) 725.
- [3] M. M. Farid, Y. Kim, and A. Kanzawa. *Transactions of ASME Journal of Solar Energy Engineering*. **112** (1990) 125.

- [4] T. Watanabe, H. Kikuchi, and A. Kanzawa. *Heat Recovery Systems & CHP*. **13** (1) (1993) 57.
- [5] M. Matsuoka, K. Tsubohara, and T. Yasukawa. *Journal of Chemical Engineering of Japan*. **21** (9) (1988) 238.
- [6] D. Feldman, D. Banu and D. Hawes. *Solar Energy Materials and Solar Cells*. **36** (1995) 311.
- [7] W. S. Kim and H. O. Song. *Journal of Chemical Engineering of Japan*. **21** (1) (1988) 69.
- [8] B. Carlsson and G. Wettermark. *Solar Energy*. **24** (1980) 239.
- [9] M. Yanadori and T. Masuda. *Solar Energy*. **42** (1) (1989) 27.
- [10] R. G. Kemink and E. M. Sparrow. *International Journal of Heat and Mass Transfer*. **24** (10) (1981) 1699.
- [11] P. Brosseau and M. Lacroix. *Fundamentals of Phase Change: Sublimation and Solidification*. ASME HTD-286 (1994) 13.
- [12] S. M. Aceves, H. Nakamura, G. M. Reistad and J. Martinez-Frias. *Transactions of the ASME- Journal of Solar Energy Engineering*. **120** (1998) 14.
- [13] M. N. R. Dimaano and A. Escoto. *ENERGY-The International Journal*. **23** (5) (1998) 421.
- [14] J. A. Banzon and A. P. Resurreccion. *The Philippine Journal of Coconut Studies*. **4** (2) (1979) 1.
- [15] K. E. Kirk and D. F. Othmer. *Encyclopedia of Chemical Technology*. **6** (1951).